A harmonic oscillator model to study the intensification of microwave radiation by a subwavelength uniform plasma discharge

Adrien Laffont,[1,2,3,a)] Romain Pascaud,[2] Thierry Callegari,[3] Laurent Liard,[3] Olivier Pascal,[3] and Jean-Pierre Adam[1]
[1)] *CEA, DAM, CEA-Gramat, 46500 Gramat, France*
[2)] *ISAE-SUPAERO, Université de Toulouse, 10 avenue Edouard Belin, 31055 Toulouse, France*
[3)] *LAPLACE, Université de Toulouse, CNRS, INPT, UPS, 118 route de Narbonne, 31062 Toulouse, France*

(Dated: 8 February 2021)

A harmonic oscillator model is proposed to study the intensification of microwave radiation of an electrically small antenna when surrounded by a subwavelength plasma discharge. This model describes the oscillations of free electrons in a spherical plasma when it is excited by an incident electromagnetic wave. It shows that at resonance, these charge oscillations lead to a significant volume current, and thus to an enhancement of the radiation. Depending on the electron density of the plasma, this radiation enhancement may occur in the microwave range. The proposed model is compared with the Mie scattering theory with perfect agreement when the electrical size *ka* of the spherical plasma remains smaller than 0.1. Despite its apparent simplicity, this model unveils the main mechanism that stands behind the intensification of microwave radiation by a subwavelength plasma discharge.

I. INTRODUCTION

Low-temperature plasmas are of particular interest for the design of new microwave antennas.[1–16] From the electromagnetic point of view, such plasmas are generally described by the Drude model of the relative permittivity ε_p. For a non-magnetized low-temperature cold plasma it is given by[17]

$$\varepsilon_p = 1 - \frac{\omega_p^2}{\omega(\omega + i\nu)}, \text{ with } \omega_p = \sqrt{\frac{e^2 n_e}{\varepsilon_0 m_e}} \quad (1)$$

where ν, ω_p, e, n_e, m_e, and ε_0 are the electron-neutral collision frequency, the plasma angular frequency, the Coulomb charge, the electron density, the electron mass, and the free space permittivity, respectively. Neglecting collisions (i.e., $\nu \ll \omega$), Eq. (1) clearly shows that such a plasma can behave either as a good electrical conductor for angular frequencies well below the plasma angular frequency (i.e., $\omega \ll \omega_p$), or as a dielectric medium when $\omega > \omega_p$.

Most of plasma-based antennas proposed in the literature use the plasma as a good electrical conductor in order to replace metallic wires or reflectors and obtain stealth, tunable, steerable, and even flexible antennas.[1–5] Directional antennas with beam steering capabilities have also been achieved by using electrically large plasmas as dielectric media.[6,7] The plasma then acts as a dielectric lens whose refractive index can be controlled to change the focus of the propagating microwave fields. Other studies have pointed out another interesting use of low-temperature plasmas for the design of electrically small antennas.[8–16] In this case, the plasma behaves neither as a good electrical conductor, nor as a dielectric, but rather as a poor electrical conductor. Several explanations have therefore been proposed to explain the intensification of the microwave radiation due to the plasma.

[a)] Electronic mail: adrien.laffont@isae-supaero.fr.

Messiaen and Vandenplas[8] have carried out one of the first experiments demonstrating the enhanced radiation of an electrically small spherical antenna when surrounded by a subwavelength plasma layer. In their work,[8] as well as in more recent studies,[9,10,12] the intensification of the microwave radiation has been justified by the tuning effect of the plasma layer on the electrically small antenna input impedance. The plasma then behaves as an inductive medium compensating for the capacitive nature of the antenna input impedance, thereby improving its radiation efficiency. Recent experimental results obtained by Laquerbe *et al.*[15] partly support this explanation. Wang *et al.*[13] have studied numerically the impact of the plasma discharge on the phase of the electric and magnetic fields in the near field region. They have suggested that the plasma layer produces a phase difference for these fields that allows enhanced radiation in the far field region. Finally, several studies have considered this microwave radiation enhancement as directly due to the resonance of the plasma itself.[11,15,16] This resonance, also known as the localized surface plasmon resonance (LSPR) in plasmonics, may thus be excited by the dipole located within it, and it is the combination of the plasma resonator with this dipole excitation that leads to an efficient electrically small antenna. It appears that the main mechanism that stand behind the intensification of microwave radiation remains misunderstood. In this paper, we propose to study it using a harmonic oscillator (HO) model.

As mentioned, the intensification of microwave radiation by a subwavelength plasma discharge and the problems addressed in plasmonics appear to be directly linked.[18–20] The LSPR is more precisely a physical phenomenon that can occur for conductive objects that are very small compared to the wavelength of the incident electromagnetic excitation.[21] In optics, the LSPR is obtained with metallic nanoparticles and used to build optical antennas.[22] Usually, the resonance condition is determined by solving an electromagnetic scattering problem under the quasi-static approximation, that is to say for objects whose electrical size tends to 0. For a lossless spherical particle, the resonance condition appears when its relative permittivity is exactly equal to -2, namely a weakly conducting medium[21]. Considering materials described by the Drude model of Eq. (1), the condition $\varepsilon_p = -2$ is then obtained for the angular frequency $\omega = \omega_p/\sqrt{3}$. Note that more accurate results can be obtained using Mie scattering theory for spheres of any realistic electrical size.[23,24] While these methods provide information on the behaviour of the LSPR, they do so with a macroscopic view of the problem using global parameters such as the relative permittivity ε_p, and one then loses the physical meaning of this resonance.

In this paper, we propose to use a harmonic oscillator (HO) model to study the intensification of radiation produced by a subwavelength gaseous plasma sphere. HO models have already been used to study metal nanoparticles.[25,26] Although very simple, these models make it possible to understand the dynamics of the plasma electrons at the mesoscopic scale during resonance and thus to bring a new perspective to the development of efficient electrically small plasma-based antennas.

II. HARMONIC OSCILLATOR MODEL

We first assume that a uniform low-temperature plasma sphere of radius a can be thought as the superposition of two rigid spheres of charged particles in a background neutral gas: one of uniform negative charge (i.e., the free electrons of density n_e) and one of uniform positive charge (i.e., the ions). Ions and neutrals are considered fixed due to their large mass, while electrons are free to move around their equilibrium position. When moving, the free electrons are assumed to mainly collide neutrals with a mean electron-neutral collision frequency ν. Since we are dealing with weakly ionized plasmas, the electron-ion collision frequency is negligible compared to the electron-neutral collision frequency. This plasma model does not take into account its containing layer which leads to a plasma sheath and its inhomogeneity. However, as discussed in Section IV, these plasma characteristics do not change the physical interpretation of the mechanisms that stand behind the radiation enhancement. Therefore, the main objective being the understanding of the physical phenomenon, a first-order description of the plasma is voluntarily considered.

Assuming that it is possible to shift by an amount $z \ll a$ the electron sphere without perturbating the internal structure of each sphere as shown in Fig. 1, a negative static surface charge appears on one pole of the sphere and a positive surface charge on the opposite pole. These surface charges produce a static electric field inside the sphere given by Gauss's law as[27]

$$\mathbf{E_{in}} = \frac{en_e}{3\varepsilon_0}\mathbf{z} \tag{2}$$

We now suddenly release the constraint on the electron sphere. By modeling the effect of the electron-neutral collisions as a frictional force $\mathbf{F_{loss}} = -m_e \nu \frac{d\mathbf{z}}{dt}$, the equation of

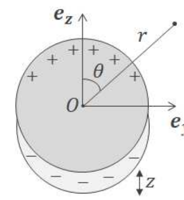

FIG. 1. 2D schematic of the disturbed plasma sphere with a plane view of the spherical coordinate system.

motion for a single electron within the sphere is given by

$$m_e \frac{d^2\mathbf{z}}{dt^2} = -e\mathbf{E_{in}} + \mathbf{F_{loss}} \tag{3}$$

that is to say

$$\frac{d^2\mathbf{z}}{dt^2} + \nu\frac{d\mathbf{z}}{dt} + \frac{{\omega_p}^2}{3}\mathbf{z} = \mathbf{0} \tag{4}$$

It corresponds to the equation of a damped harmonic oscillator whose angular resonant frequency is the so-called Mie frequency $\omega_p/\sqrt{3}$. Note that geometries other than the spherical geometry can be modeled if the analytical expression of the restoring force is known. Then, the resonance condition will certainly be different. For example, for a bulk plasma we obtain the well known plasmon resonance for $\omega = \omega_p$.[21]

So far, these results are not directly related to our antenna problem. When dealing with an electrically small antenna surrounded by a subwavelength plasma layer, an additional external force is applied to the free electrons corresponding to the electromagnetic field radiated by the source inside the plasma within the transmitting mode. However, the model may be complicated depending on the feeding system. As a result, it is proposed to study the plasma sphere when illuminated by an electromagnetic linearly polarized plane wave as done in plasmonics.[21] In practice, this is equivalent to studying the unloaded plasma resonator.[28] The question of coupling between this resonator and the feeding system is thus set aside.[29]

We now consider that the plasma sphere is illuminated by an electromagnetic linearly polarized plane wave propagating in the y-direction with the electric field in the z-direction. The sphere is centered at the origin of the coordinate system and assumed to be very small compared to the wavelength of the incident plane wave ($a \ll \lambda$). As a result, the electromagnetic field seen by the entire sphere is almost uniform. The ky-dependence, with $k = 2\pi/\lambda$ the wave vector, in the plane wave expression can be neglected and the external driving force applied to each free electron in the plasma is

$$\mathbf{F_{ext}} = -e\mathbf{E_{inc}}, \text{ with } \mathbf{E_{inc}} = E_0\cos(\omega t + \phi)\mathbf{e_z} \tag{5}$$

where ω is the angular frequency of the wave and ϕ its phase at the origin. Thus, we obtain the equation of a driven HO with a cosinusoidal driving force

$$\frac{d^2\mathbf{z}}{dt^2} + \nu\frac{d\mathbf{z}}{dt} + \frac{{\omega_p}^2}{3}\mathbf{z} = -\frac{eE_0}{m_e}\cos(\omega t + \phi)\mathbf{e_z} \tag{6}$$

Note that since we are dealing with charged particles in motion, we could have considered losses due to electromagnetic radiation through the radiation reaction force also known as Abraham-Lorentz force.[26] However, these losses are negligible at microwave frequencies compared to collision losses.[27]

In steady state, the electrons oscillate around their equilibrium position. Assuming a harmonic time dependence factor $e^{i\omega t}$, such that $\mathbf{z}(t) = \mathrm{Re}[\mathbf{Z}e^{i\omega t}]$, a particular solution of Eq. (6) is given by

$$\mathbf{Z} = \frac{eE_0e^{i\phi}/m_e}{(\omega^2 - \frac{{\omega_p}^2}{3}) - i\omega\nu}\mathbf{e_z} \tag{7}$$

All the free electrons now contribute to a macroscopic uniform current $\mathbf{J} = -en_e i\omega\mathbf{Z}$ within the sphere, such that

$$\mathbf{J} = J_z\mathbf{e_z} = \frac{-i\omega{\omega_p}^2\varepsilon_0E_0e^{i\phi}}{(\omega^2 - \frac{{\omega_p}^2}{3}) - i\omega\nu}\mathbf{e_z} \tag{8}$$

This induced current is then responsible for radiation or more precisely for a scattered electromagnetic field. This field can be calculated using the vector potential $\mathbf{A}$. Consider a spherical polar (r,θ,φ) coordinate system with r the distance to the center, θ the polar angle, and φ the azimuthal angle (see Fig. 1. Since $a \ll \lambda$, the vector potential $\mathbf{A}$ is defined at any point outside the sphere $r > R$ as[29,30]

$$\mathbf{A} = \frac{\mu_0}{4\pi}\frac{e^{-ikr}}{r}\iiint_V \mathbf{J}\,dV = \frac{\mu_0 a^3 e^{-ikr}}{3r}\mathbf{J} \tag{9}$$

as the current $\mathbf{J}$ is uniform within the sphere. Here, μ_0 and V are the free space permeability and the volume of the sphere, respectively. The scattered electric field $\mathbf{E_{sca}}$ in the far-field region is given by $-i\omega\mathbf{A}$[29,30]

$$\mathbf{E_{sca}} = \frac{a^3E_0e^{i\phi}}{3c^2}\frac{\omega^2{\omega_p}^2}{[(\omega^2 - \frac{{\omega_p}^2}{3}) - i\omega\nu]}\frac{\sin(\theta)e^{-ikr}}{r}\mathbf{e}_\theta \tag{10}$$

Note here that it corresponds to the radiation pattern of a small dipole with a maximum for $\theta = \pm\pi/2$.

From Eq. (10) we can also derive the bistatic radar cross section (RCS) σ of the sphere which is a metric on its ability to scatter electromagnetic energy in a given direction when illuminated by an incident wave[30]

$$\sigma = \lim_{r\to+\infty}[4\pi r^2\frac{|\mathbf{E_{sca}}|^2}{|\mathbf{E_{inc}}|^2}] \tag{11}$$

that is to say

$$\sigma = \frac{4\pi a^6{\omega_p}^4}{9c^4}\frac{\omega^4}{[(\omega^2 - \frac{{\omega_p}^2}{3})^2 + \omega^2\nu^2]}\sin^2(\theta) \tag{12}$$

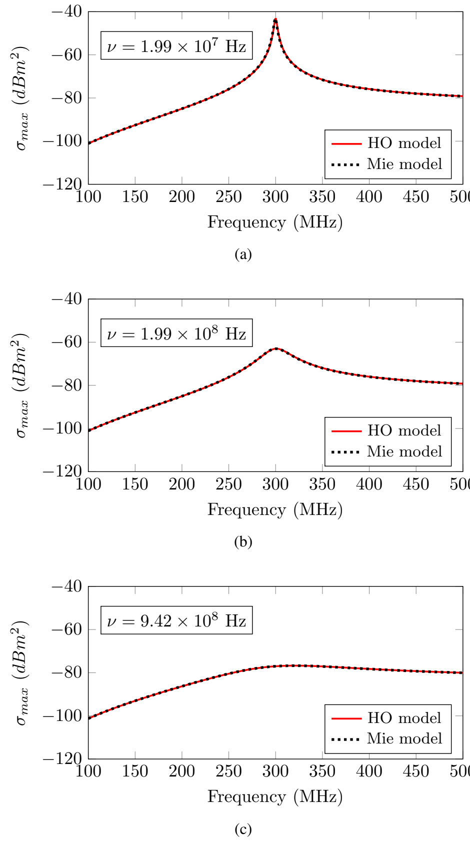

FIG. 2. Maximum RCS of a plasma sphere ($n_e = 3.35 \times 10^9$ cm^{-3}) with $ka = 0.05$ at 300 MHz ($a = 8$ mm) as a function of the frequency of the incident electromagnetic plane wave for different collision frequencies; (a) $\nu = 0.01\omega$ at 300 MHz ($\nu = 1.99 \times 10^7$ Hz); (b) $\nu = 0.1\omega$ at 300 MHz ($\nu = 1.99 \times 10^8$ Hz); (c) $\nu = 0.5\omega$ at 300 MHz ($\nu = 9.42 \times 10^8$ Hz).

III. VALIDATION OF THE MODEL

For a collisionless plasma (i.e., $\nu = 0$ Hz), we can observe from Eq. (12) that σ is maximum for $\omega = \omega_p/\sqrt{3}$. This result agrees with the solution obtained when analyzing directly the problem as an electromagnetic scattering one under quasi-static assumption.[21] However, when losses are taken into account, the RCS is maximum for a slightly higher angular frequency, or blue-shifted

$$\omega = \frac{{\omega_p}^2}{3}\left(\frac{{\omega_p}^2}{3} - \frac{\nu^2}{2}\right)^{-1/2} \tag{13}$$

When losses are taken into account, the results of the HO model must be compared with an electromagnetic numerical code. In the case of spherical geometry, general Mie scattering theory is particularly suitable for simulating the problem by considering a sphere of a material defined by the Drude model.[23,24,31] The results of the HO model are thus compared with an in-house software exploiting Mie scattering theory, details of which have been published by Shore.[24] The HO model assumes $a \ll \lambda$, whereas Mie theory remains valid for any electrical size ka of the sphere. We first model a plasma sphere such that its electrical size ka is equal to 0.05 at 300 MHz, namely $a = 8$ mm. To obtain the LSPR at 300 MHz we must then have $n_e = 3.35 \times 10^9$ cm^{-3} if $\nu \ll \omega$. These plasma parameters were arbitrarily chosen to refer to previous experimental work on electrically small plasma-based antennas.[15]

Figures 2a shows the maximum value for the RCS of the plasma sphere σ_{max} calculated analytically with the HO model and numerically with the Mie model. A low collision frequency $\nu = 0.01\omega$ at 300 MHz (i.e., $\nu = 1.88 \times 10^7$ Hz) is here considered. These curves clearly show that the HO model is consistent with the results obtained using the in-house Mie software. As plasma losses increase, a decrease in σ_{max} is observed as well as a frequency shift of its maximum value. Figures 2b and 2c present the maximum value for the RCS considering the same dimensions for the spheres as in Fig. 2a but with larger collision frequencies $\nu = 0.1\omega$ (i.e., $\nu = 1.99 \times 10^8$ Hz) and $\nu = 0.5\omega$ at 300 MHz (i.e., $\nu = 9.42 \times 10^8$ Hz), respectively. We note that the microwave radiation enhancement decreases and that the resonant frequency is blue-shifted from 0.8 MHz and 20 MHz, respectively, which is in agreement with Eq. (13).

If Mie scattering theory can be used for a sphere of any size, it is important to note that the HO model is only valid when the electrical size ka of the plasma sphere is sufficiently small, that is to say when the quasi-static approximation holds.[31] Figure 3a thus recalls σ_{max} for $ka = 0.05$ (i.e., $a = 8$ mm), while Fig. 3b and 3c refer to larger spheres with $ka = 0.2$ (i.e., $a = 32$ mm) and $ka = 0.5$ (i.e., $a = 80$ mm), respectively, also considering $\nu = 0.01\omega$ at 300 MHz. Besides, graphical inserts in Fig. 3 show precisely the scale ratio between the plasma sphere (black dot) and the wavelength at 300 MHz. As the electrical size ka of the sphere increases, the HO model fails to predict both the frequency and intensity of the resonance peak. If ka is too large, the electrons no longer oscillate coherently because the incident electromagnetic field is no longer uniform inside the plasma, and the driving force of the HO model does not take it into account.

Figure 4 gives the error made with the HO model on the resonant frequency f_{res} as a function of the electrical size ka for $n_e = 3.35 \times 10^9$ cm^{-3} with three collision frequencies $\nu = 0.01\omega$ (i.e., $\nu = 1.99 \times 10^7$ Hz), $\nu = 0.1\omega$ (i.e., $\nu = 1.99 \times 10^8$ Hz), and $\nu = 0.5\omega$ (i.e., $\nu = 9.42 \times 10^8$ Hz) at 300 MHz. An error of less than 10 % is observed as long as $ka \leqslant 0.5$.

Concerning the magnitude of σ_{max} at resonance, Fig. 5 shows the difference in dB between the two peaks for $n_e = 3.35 \times 10^9$ cm^{-3} with three collision frequencies $\nu = 0.01\omega$, $\nu = 0.1\omega$, and $\nu = 0.5\omega$ at 300 MHz. When losses are low, a large discrepancy can be observed between the HO model and the Mie code as ka increases. However, an increase in losses within the plasma tends to reduce this deviation.

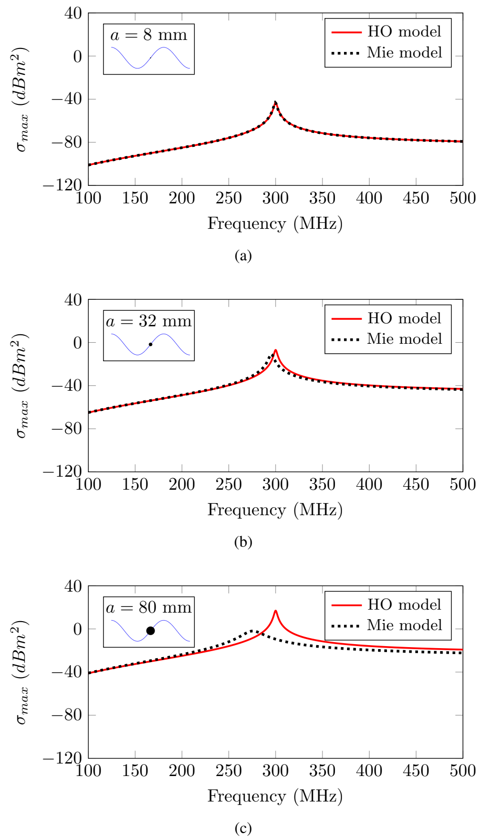

FIG. 3. Maximum RCS of a plasma sphere ($n_e = 3.35 \times 10^9$ cm^{-3} and $\nu = 1.99 \times 10^7$ Hz) as a function of the frequency of the incident electromagnetic plane wave for different electrical size; (a) $ka = 0.05$ at 300 MHz ($a = 8$ mm); (b) $ka = 0.2$ at 300 MHz ($a = 32$ mm); (c) $ka = 0.5$ at 300 MHz ($a = 80$ mm).

In order to keep an error on the resonant frequency f_{res} of less than 1 % and a deviation on the amplitude of σ_{max} of less than 1 dB we need to have $ka \leqslant 0.1$. This value, although arbitrary, gives an idea of the range of validity of the HO model.

IV. DISCUSSION

According to the HO model, we can state that the intensification of the electromagnetic field due to an electrically small

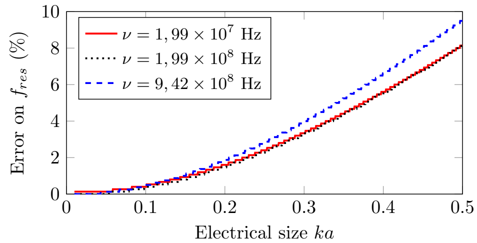

FIG. 4. Error on the resonant frequency f_{res} between the HO and Mie models as a function of the electrical size ka for three collision frequencies $\nu = 0.01\omega$ ($\nu = 1.99 \times 10^7$ Hz), $\nu = 0.1\omega$ ($\nu = 1.99 \times 10^8$ Hz), and $\nu = 0.5\omega$ ($\nu = 9.42 \times 10^8$ Hz) at 300 MHz.

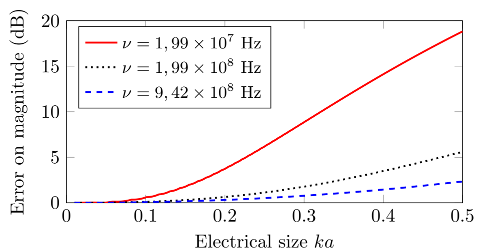

FIG. 5. Difference (dB) for peaks intensity of the maximum RCS between the HO and Mie models as a function of the electrical size ka for three collision frequencies $\nu = 0.01\omega$ ($\nu = 1.99 \times 10^7$ Hz), $\nu = 0.1\omega$ ($\nu = 1.99 \times 10^8$ Hz), and $\nu = 0.5\omega$ ($\nu = 9.42 \times 10^8$ Hz) at 300 MHz.

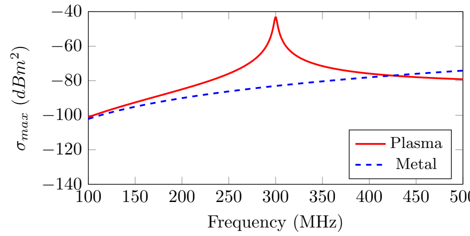

FIG. 6. Maximum RCS of plasma ($n_e = 3.35 \times 10^9$ cm^{-3} and $\nu = 1.99 \times 10^7$ Hz) and metal spheres ($n_e = 10^{22}$ cm^{-3} and $\nu = 10^{14}$ Hz) with radius $ka = 0.05$ at 300 MHz ($a = 8$ mm) as a function of the frequency of the incident electromagnetic plane wave.

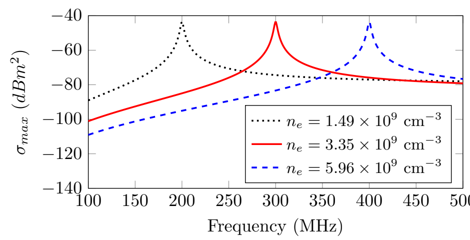

FIG. 7. Maximum RCS of a plasma sphere of radius $a = 8$ mm for three electron densities $n_e = 1.49 \times 10^9$ cm^{-3}, $n_e = 3.35 \times 10^9$ cm^{-3}, and $n_e = 5.96 \times 10^9$ cm^{-3}, and considering $\nu = 1.99 \times 10^7$ Hz, as a function of the incident plane wave frequency.

plasma spherical discharge results from a collective oscillation of the free electrons inside the plasma. This oscillation leads to a volume current $\mathbf{J}$ that emits intense microwave radiation at resonance. However, it is important to notice that this resonance is only obtained for very specific conditions.

For instance, Fig. 6 shows the maximum value for the RCS calculated with the HO model for plasma and metal spheres of electrical sizes $ka = 0.05$ at 300 MHz. For the metal sphere we consider conventional metals, such as silver or gold, for which we have $n_e \sim 10^{22}$ cm^{-3} and $\nu \sim 10^{14}$ Hz.[32] Although these conventional metals are conducting materials in which free electrons are susceptible to be set in motion, we note in Fig. 6 that their electron density is too high to achieve the resonance condition at the frequency of interest, namely 300 MHz. Regarding the losses, they have to remain small enough to exhibit a sharp resonance as already shown in Fig. 2. For instance, higher losses as in Fig. 2c leads to a great reduction of the intensity of the resonance. Finally, in order to obtain a resonance phenomenon at a particular microwave frequency, the electron density and collision frequency must be controlled and not all conducting materials can be used. Within a plasma discharge, it is possible to control these parameters to certain extent in order to obtain resonance for instance at 300 MHz (e.g., $n_e = 3.35 \times 10^9$ cm^{-3} and $\nu = 1.99 \times 10^7$ Hz in Fig. 6).

It is also interesting to notice that one can theoretically control the resonant frequency of the plasma sphere by modifying its electron density. For example, Fig. 7 shows σ_{max} as a function of the incident plane wave frequency for a plasma sphere of radius $a = 8$ mm for three different electron densities $n_e = 1.49 \times 10^9$ cm^{-3}, $n_e = 3.35 \times 10^9$ cm^{-3}, and $n_e = 5.96 \times 10^9$ cm^{-3}, and considering $\nu = 1.99 \times 10^7$ Hz.

We clearly observe a decrease of the resonant frequency when the electron density decreases. Note that for each case $ka \leqslant 0.1$ and therefore the HO model remains valid. Controlling the resonant frequency of the plasma resonator is an interesting feature that may be used to design frequency tunable electrically small antennas as already demonstrated in our previous work.[15]

The results presented in this paper should be considered keeping in mind the limitations of the proposed model, particularly with regard to the description of the plasma itself. Indeed, here the plasma is assumed to be perfectly spherical, uniform, and in free space, whereas in practice it is confined in a containment layer which leads to its inhomogeneity as well as to the presence of a plasma sheath.[15] However, the containing layer and plasma sheath simply behave as additional dielectric layers which are known to only produce a shift of the resonant frequency.[33] Besides, such a frequency shift has also been observed in studies on the effect of the inhomogeneity of spherical objects.[34] Finally, although plasma real characteristics may modify its resonant frequency, they do not modify the physical phenomenon that stands behind the intensification of microwave radiation and that is unveiled by the proposed HO model.

V. CONCLUSION

A simple harmonic oscillator (HO) model has been proposed to unveil the main mechanism responsible for the intensification of microwave radiation by an electrically small antenna when surrounded by a subwavelength plasma discharge. The results from the HO model are consistent with that calculated with a Mie code while the electrical size of the sphere ka remains lower than 0.1. From this HO model we can conclude that:

- in a sub-wavelength plasma discharge, collective oscillations of its free electrons arise when they are driven by an external incident electromagnetic field,
- the intensification of the microwave radiation is due to the resonance of these collective oscillations, also known as localized surface plasmon resonance (LSPR), that leads to a large volume current and thus an enhanced radiated electromagnetic field,
- the resonant frequency depends mostly on the plasma electron density when the collision frequency is small compared to the angular frequency of the incident electromagnetic field,
- the resonant frequency is also a function of the shape of the plasma discharge and of the properties of the incident electromagnetic field (i.e., angle of incidence and polarization) through its induced surface charge density distributions that establish the restoring force,
- the resonance tends to vanish for large collision frequency due to power dissipation within the plasma,
- the resonance tends to vanish for large electrical size of the plasma because the electrons no longer oscillate coherently,
- frequency tunability of the resonance can be achieved by controlling the electron density of the plasma.

This HO model finally gives an intuitive understanding of the main mechanism occurring inside the plasma that is responsible for the intensification of the microwave radiation.

ACKNOWLEDGMENTS

The authors would like to thank the Direction Générale de l'Armement (DGA), the Agence de l'Innovation de Défense (AID), and the Région Occitanie for their financial support.

DATA AVAILABILITY

The data that support the findings of this study are available from the corresponding author upon reasonable request.

REFERENCES

[1] G. G. Borg, J. H. Harris, N. M. Martin, D. Thorncraft, R. Milliken, D. G. Miljak, B. Kwan, T. Ng, and J. Kircher, "Plasmas as antennas: Theory, experiment and applications," Phys. Plasmas **7**, 2198–2202 (2000).
[2] I. Alexeff, T. Anderson, S. Parameswaran, E. P. Pradeep, J. Hulloli, and P. Hulloli, "Experimental and theoretical results with plasma antennas," IEEE Trans. Plasma Sci. **34**, 166–172 (2006).
[3] M. T. Jusoh, O. Lafond, F. Colombel, and M. Himdi, "Performance and radiation patterns of a reconfigurable plasma corner-reflector antenna," IEEE Antennas Wireless Propag. Lett. **12**, 1137–1140 (2013).
[4] Y. P. Bliokh, J. Felsteiner, and Y. Z. Slutsker, "X-band microwave antenna with a switchable planar plasma reflector," J. Appl. Phys. **120**, 113301 (2016).
[5] J. Zhao, S. Wang, H. Wu, Y. Liu, Y. Chang, and X. Chen, "Flexible plasma linear antenna," Appl. Phys. Lett. **110**, 094108 (2017).
[6] P. Linardakis, G. Borg, and N. Martin, "Plasma-based lens for microwave beam steering," Electron. Lett. **42**, 444–446 (2006).
[7] J. Sokoloff, A. Kallel, and T. Callegari, "Reconfigurable leaky wave antenna using a gradient index plasma," in *9th European Conference on Antennas and Propagation (EuCAP)* (2015) pp. 1–5.
[8] A. M. Messiaen and P. E. Vandenplas, "Theory and experiments of the enhanced radiation from a plasma-coated antenna," Electron. Lett. **3**, 26–27 (1967).
[9] C. C. Lin and K. M. Chen, "Improved radiation from a spherical antenna by overdense plasma coating," IEEE Trans. Antennas Propag. **17**, 675–678 (1969).
[10] R. W. Ziolkowski and A. Erentok, "Metamaterial-based efficient electrically small antennas," IEEE Trans. Antennas Propag. **54**, 2113–2130 (2006).
[11] H. R. Stuart and A. Pidwerbetsky, "Electrically small antenna elements using negative permittivity resonators," IEEE Trans. Antennas Propag. **54**, 1644–1653 (2006).
[12] X. Gao, C. Wang, B. Jiang, and Z. Zhang, "A physical model of radiated enhancement of plasma-surrounded antenna," Phys. Plasmas **21**, 093301 (2014).
[13] C. Wang, H. Liu, X. Li, and B. Jiang, "The mecanism of the effect of a plasma layer with negative permittivity on the antenne radiation field," Phys. Plasmas **22**, 063501 (2015).
[14] F. R. Kong, Y. F. Sun, S. Lin, Q. Y. Nie, Z. B. Wang, Z. L. Zhang, B.-W. Li, and B. H. Jiang, "Experimental studies on radiation intensification in gigahertz radio frequency band by subwavelength plasma structures," IEEE Trans. Plasma Sci. **45**, 381–387 (2017).
[15] V. Laquerbe, R. Pascaud, A. Laffont, T. Callegari, L. Liard, and O. Pascal, "Towards antenna miniaturization at radio frequencies using plasma discharges," Phys. Plasmas **26**, 033509 (2019).
[16] B.-W. Li, Q. Nie, X. Wang, S. Lin, P. Chen, and B. Qu, "Intensification of microwave radiation by hybridized plasmon effect," Phys. Plasmas **27**, 040701 (2020).
[17] M. A. Lieberman and A. J. Lichtenberg, *Principles of Plasma Discharges and Materials Processing* (John Wiley & Sons, 2005).
[18] A. E. Rider, K. Ostrikov, and S. A. Furman, "Plasmas meet plasmonics: Everything old is new again," Eur. Phys. J. D **66**, 226–245 (2012).

[19] G. Manfredi, "Preface to special topic: Plasmonics and solid state plasmas," Phys. Plasmas **25**, 031701 (2018).
[20] R. A. Colón Quiñones, T. C. Underwood, and M. A. Cappelli, "Laser-produced gaseous plasmonic resonators," Physics of Plasmas **25**, 113501 (2018).
[21] S. A. Maier, *Plasmonics: Fundamentals and Applications* (Springer, 2007).
[22] M. Agio and A. Alù, *Optical Antennas* (Cambridge University Press, 2013).
[23] C. F. Bohren and D. R. Huffman, *Absorption and Scattering of Light by Small Particles* (John Wiley & Sons, 1998).
[24] R. A. Shore, "Scattering of an electromagnetic linearly polarized plane wave by a multilayered sphere," IEEE Antennas Propag. Mag. **57**, 69–116 (2015).
[25] J. Zuloaga and P. Nordlander, "On the energy shift between near-field and far-field peak intensities in localized plasmon systems," Nano Lett. **11**, 1280–1283 (2011).
[26] M. A. Kats, N. Y, P. Genevet, Z. Gaburro, and F. Capasso, "Effect of radiation damping on the spectral response of plasmonic components," Opt. Express **19**, 21748–21753 (2011).
[27] J. D. Jackson, *Classical Electrodynamics, 3th Edition* (John Wiley & Sons, 1998).
[28] D. M. Pozar, *Microwave Engineering, 4th Edition* (John Wiley & Sons, 2011).
[29] C. A. Balanis, *Antenna Theory: Analysis and Design, 4th Edition* (John Wiley & Sons, 2016).
[30] C. A. Balanis, *Advanced Engineering Electromagnetics, 2nd Edition* (John Wiley & Sons, 2012).
[31] Z. Mei, T. K. Sarkar, and M. Salazar-Palma, "A study of negative permittivity and permeability for small sphere," IEEE Antennas Wireless Propag. Lett. **12**, 1228–1231 (2013).
[32] A. Boltasseva and H. A. Harry, "Low-loss plasmonic metamaterials," Science **331**, 290–291 (2011).
[33] V. Laquerbe, R. Pascaud, T. Callegari, L. Liard, and O. Pascal, "Preliminary study on the feasibility of a plasma-based electrically small eng antenna," in *2016 10th European Conference on Antennas and Propagation (EuCAP)* (2016) pp. 1–5.
[34] V. Laquerbe, R. Pascaud, T. Callegari, L. Liard, and O. Pascal, "Analytical model to study the electrostatic resonance of subwavelength radially inhomogeneous negative permittivity spheres," IEEE Antennas and Wireless Propag. Letters **16**, 2894–2897 (2017).

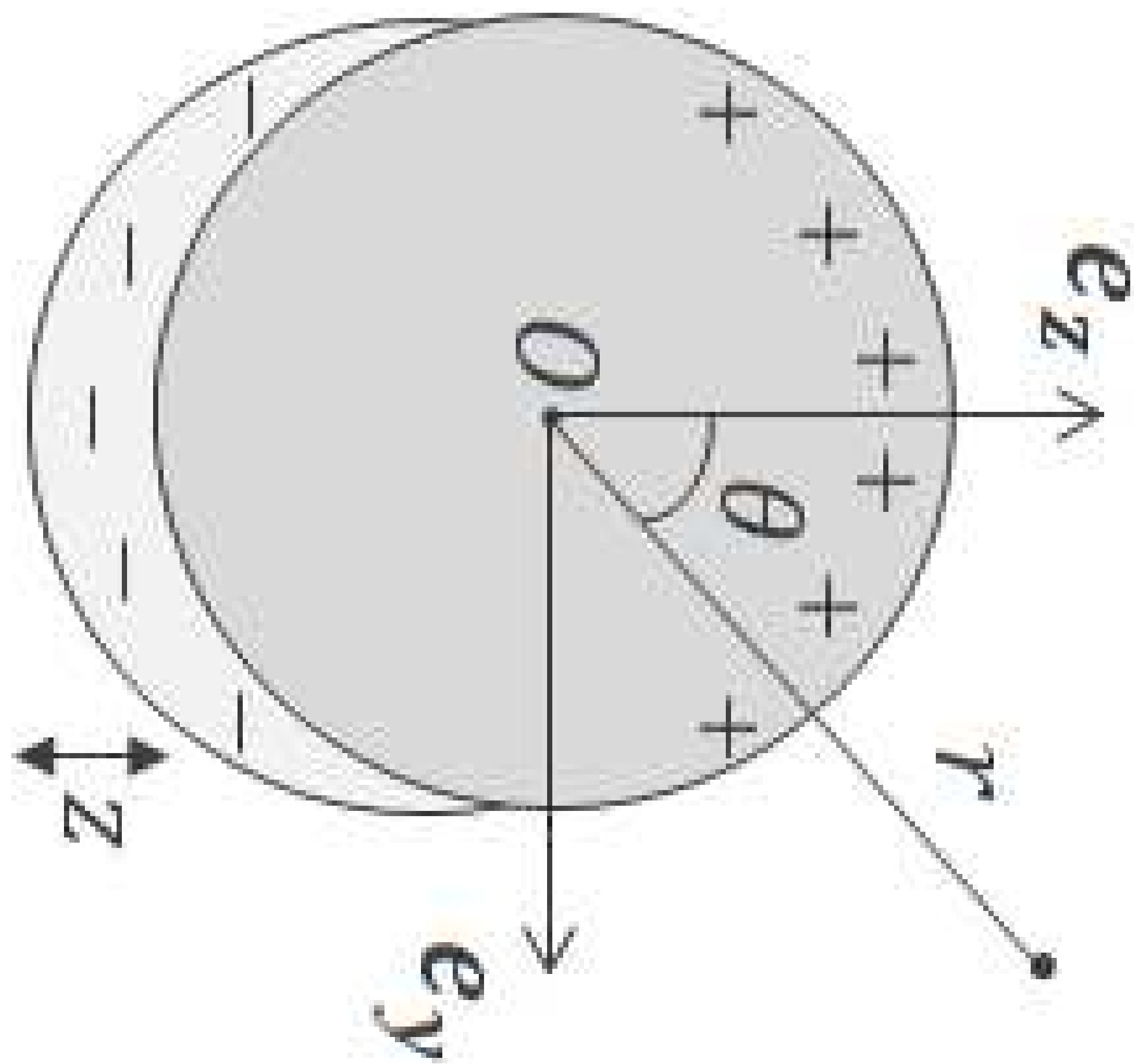
e_z
e_y
O
θ
r
z
+ + + + + + +
− − − − − −

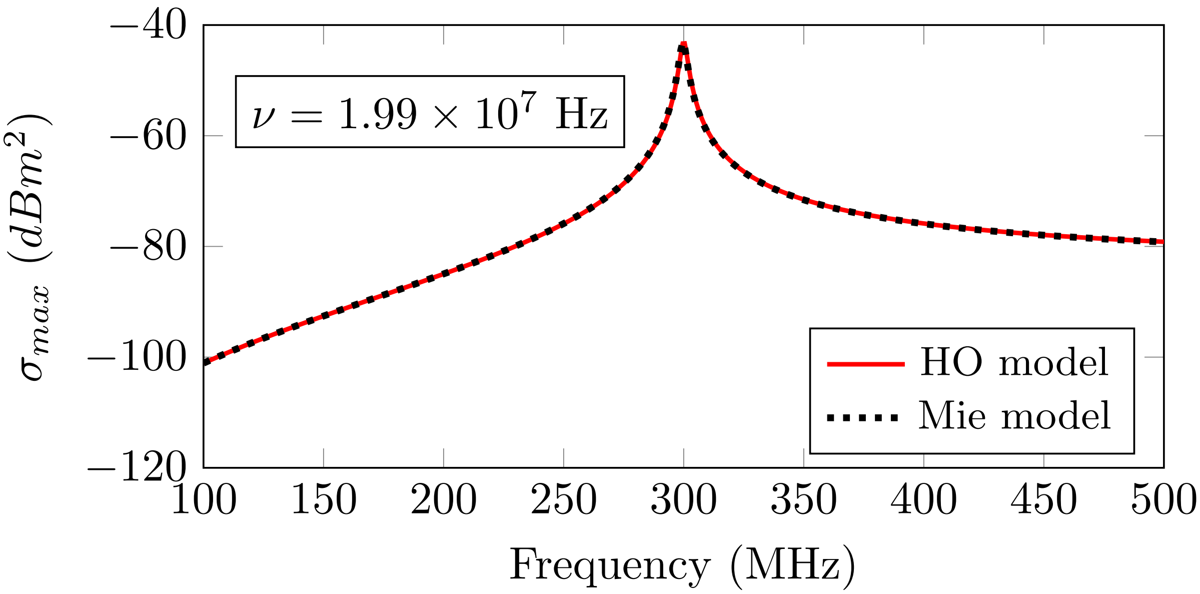
$\nu = 1.99 \times 10^7$ Hz
HO model
Mie model
σ_{max} (dBm^2)
Frequency (MHz)
−40
−60
−80
−100
−120
100
150
200
250
300
350
400
450
500

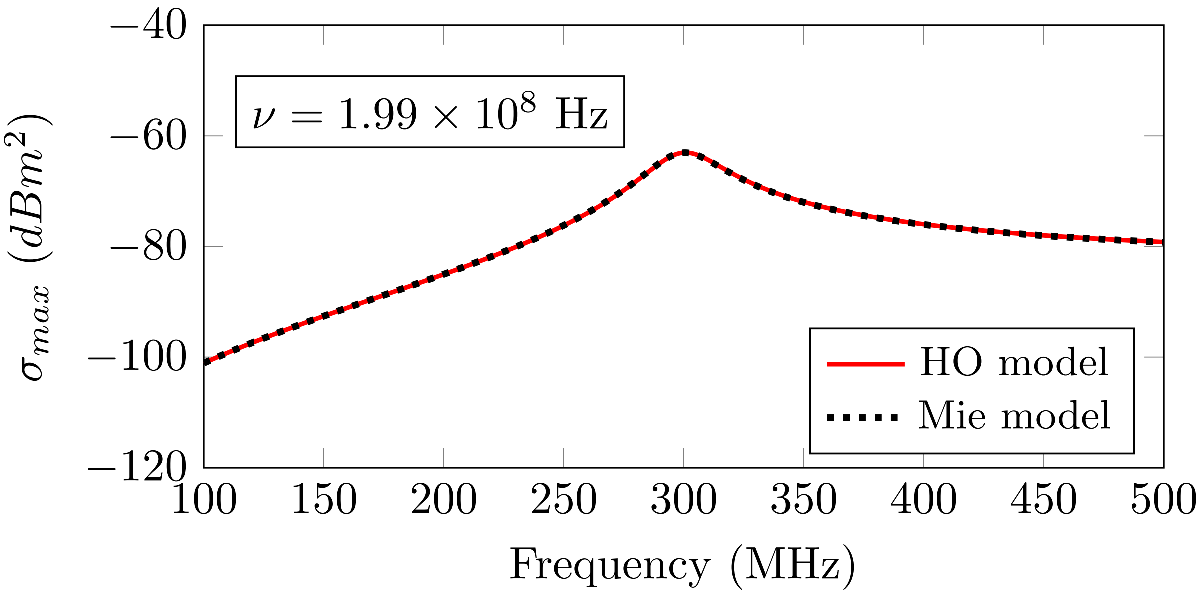
$\nu = 1.99 \times 10^8$ Hz
HO model
Mie model
σ_{max} (dBm^2)
−40
−60
−80
−100
−120
100
150
200
250
300
350
400
450
500
Frequency (MHz)

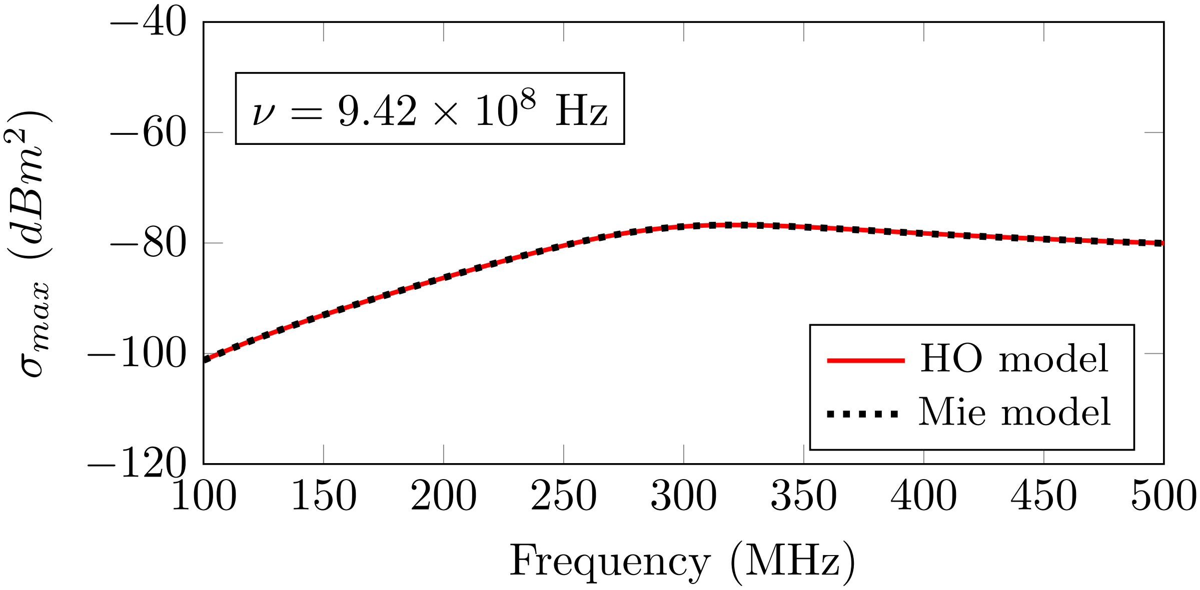
$\nu = 9.42 \times 10^8$ Hz
σ_{max} (dBm^2)
−40
−60
−80
−100
−120
100
150
200
250
300
350
400
450
500
Frequency (MHz)
HO model
Mie model

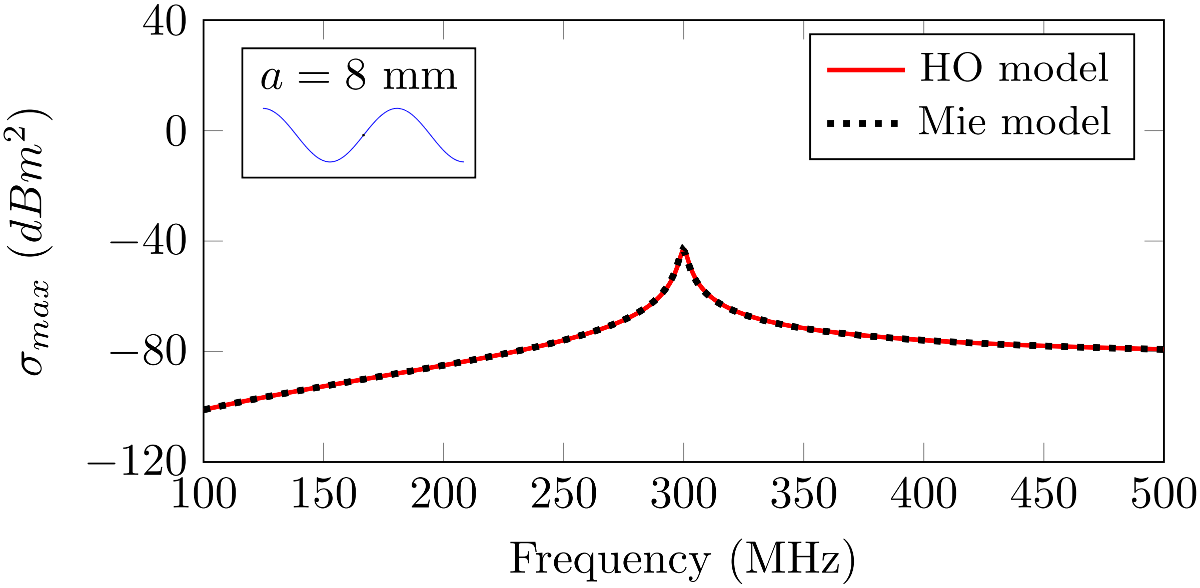
$a = 8$ mm
HO model
Mie model
40
0
−40
−80
−120
σ_{max} (dBm^2)
100
150
200
250
300
350
400
450
500
Frequency (MHz)

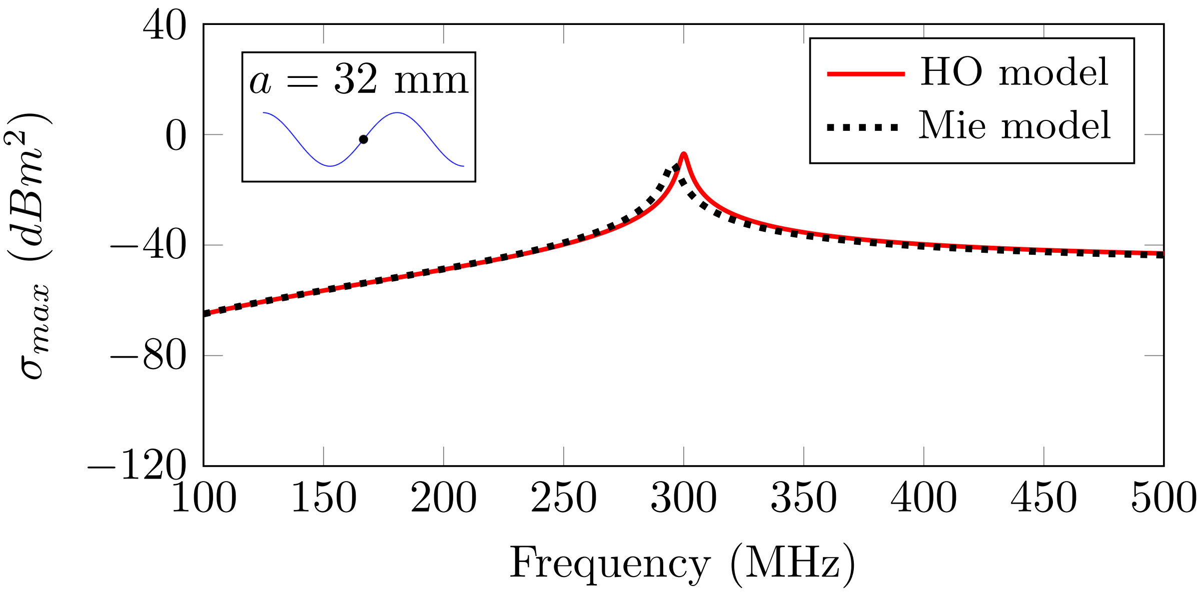
a = 32 mm
HO model
Mie model
40
0
−40
−80
−120
100
150
200
250
300
350
400
450
500
σmax (dBm2)
Frequency (MHz)

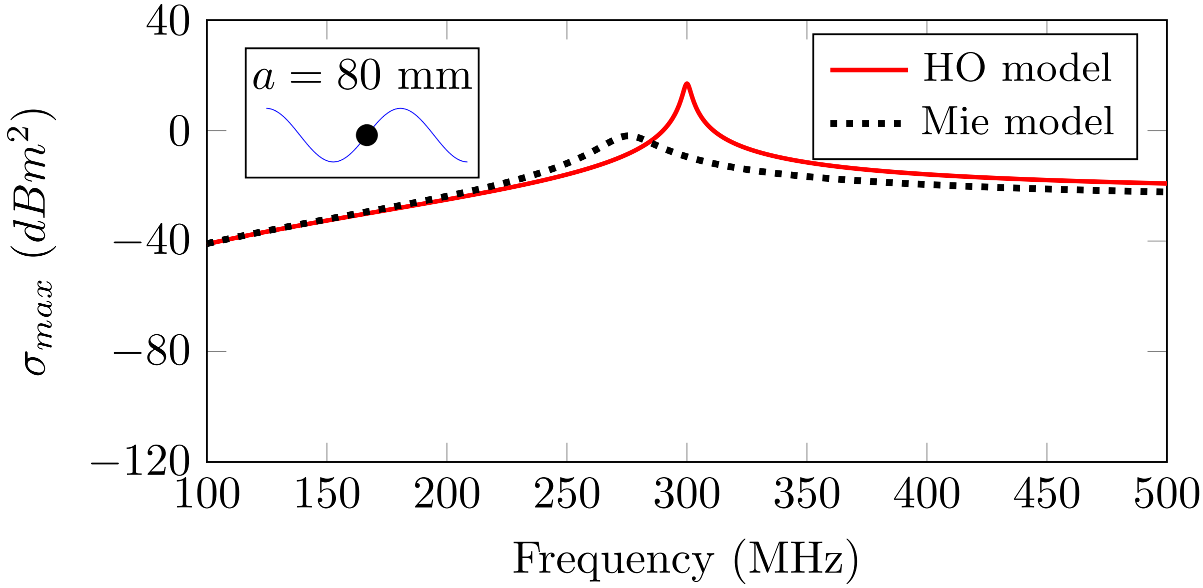
$a = 80$ mm
HO model
Mie model
σ_{max} (dBm^2)
40
0
−40
−80
−120
100
150
200
250
300
350
400
450
500
Frequency (MHz)

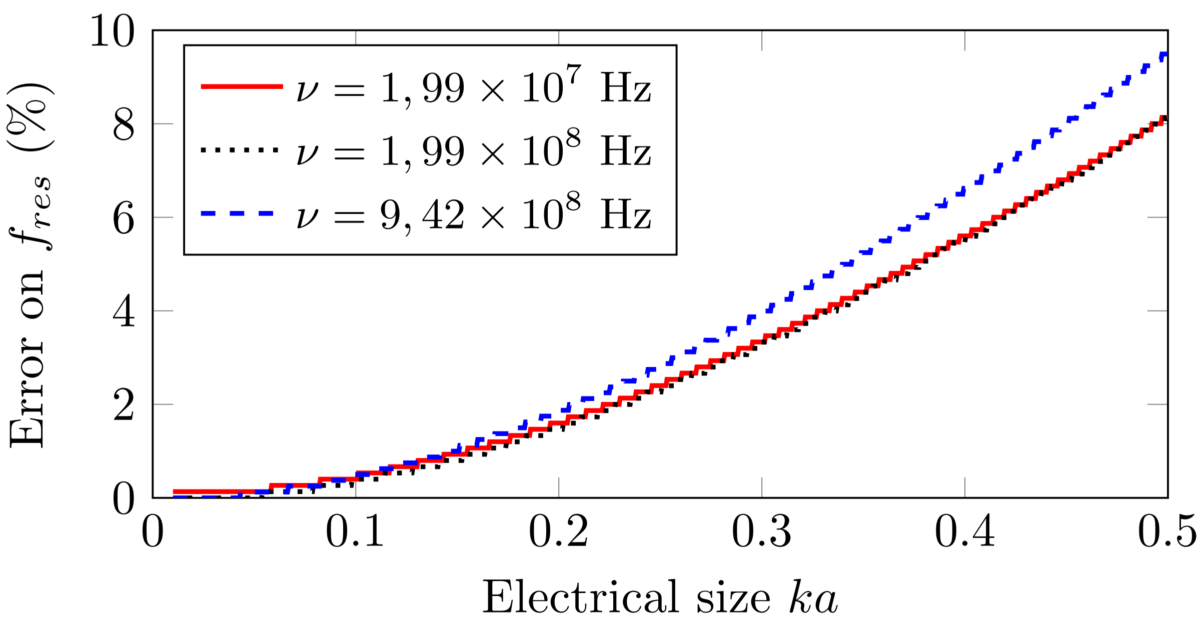
$\nu = 1,99 \times 10^7$ Hz
$\nu = 1,99 \times 10^8$ Hz
$\nu = 9,42 \times 10^8$ Hz
Error on f_{res} (%)
Electrical size ka
0
2
4
6
8
10
0
0.1
0.2
0.3
0.4
0.5

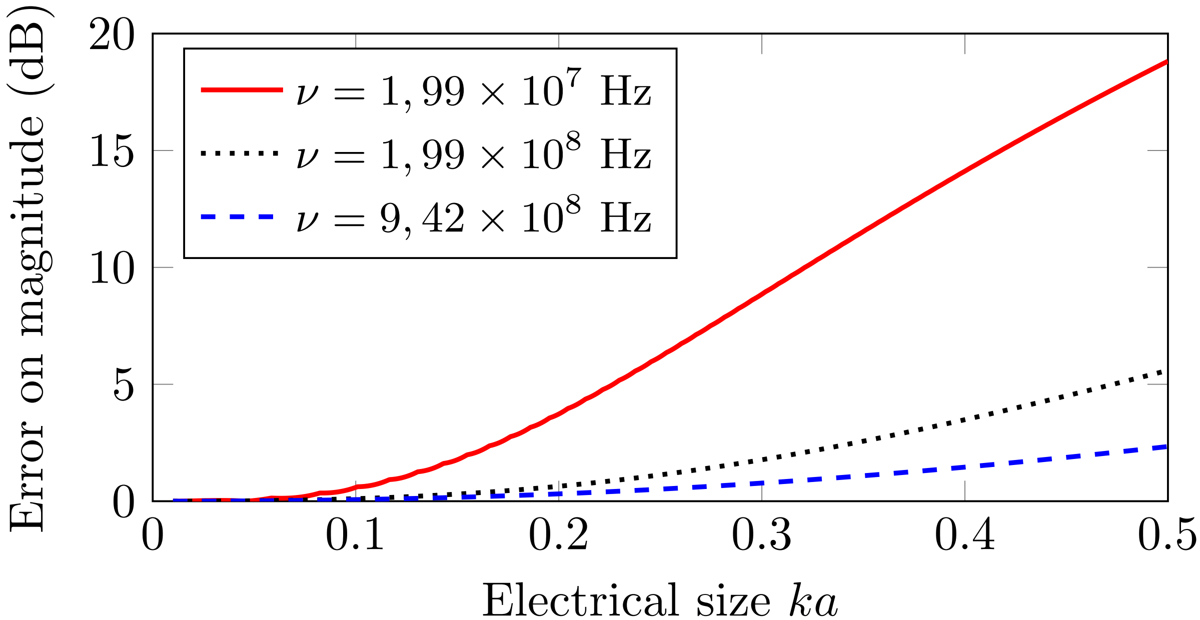
$\nu = 1,99 \times 10^7$ Hz
$\nu = 1,99 \times 10^8$ Hz
$\nu = 9,42 \times 10^8$ Hz
Error on magnitude (dB)
Electrical size ka
0
5
10
15
20
0
0.1
0.2
0.3
0.4
0.5

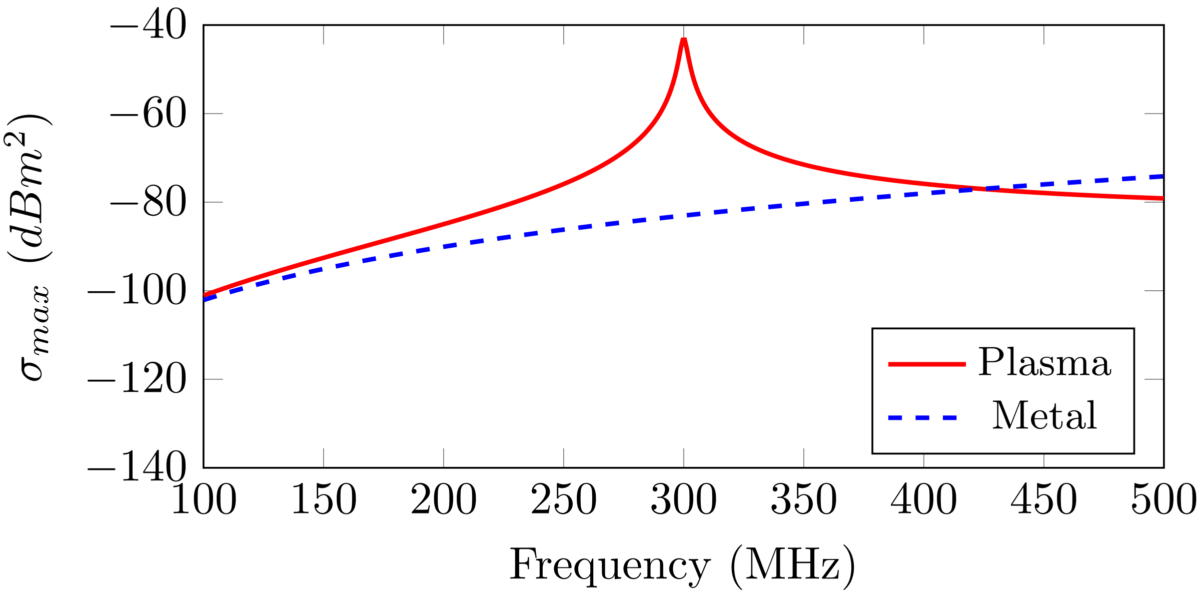
$\sigma_{max}\ (dBm^2)$
−40
−60
−80
−100
−120
−140
100
150
200
250
300
350
400
450
500
Frequency (MHz)
Plasma
Metal

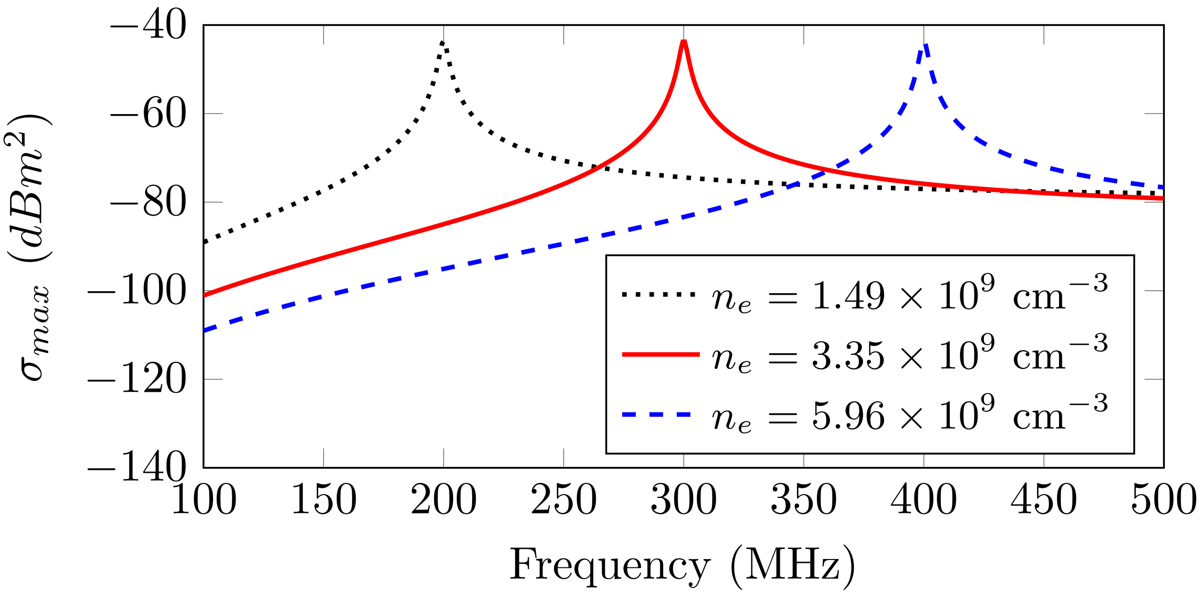
−40
−60
−80
−100
−120
−140
σ_{max} (dBm^2)
100 150 200 250 300 350 400 450 500
Frequency (MHz)
$n_e = 1.49 \times 10^9$ cm^{-3}
$n_e = 3.35 \times 10^9$ cm^{-3}
$n_e = 5.96 \times 10^9$ cm^{-3}